

1 **Emerging impacts of enhanced Greenland melting on**  
2 **Labrador Sea dynamics**

3 **Ilana Schiller-Weiss<sup>1</sup>, Torge Martin<sup>1</sup>, Franziska U. Schwarzkopf<sup>1</sup>**

4 <sup>1</sup>GEOMAR Helmholtz Centre for Ocean Research Kiel, Kiel, Germany

5 **Key Points:**

- 6 • The West Greenland Current (WGC) freshens and cools with the observed recent  
7 increase in meltwater runoff from Greenland  
8 • The density gradient across the boundary current intensifies, strengthening the  
9 WGC and increasing local eddy formation  
10 • Deep mixing of meltwater at shallower depths in the Labrador Sea contributes a  
11 shift in deep convection into the Irminger Sea (2015–2018)

---

Corresponding author: Ilana Schiller-Weiss, [ischiller-weiss@geomar.de](mailto:ischiller-weiss@geomar.de)

## Abstract

Freshwater input from Greenland ice sheet melt has been increasing in the past decades from warming temperatures. To identify the impacts from enhanced meltwater input into the subpolar North Atlantic from 1997–2021, we use output from two nearly identical simulations in the eddy-rich model VIKING20X ( $1/20^\circ$ ) only differing in the freshwater input from Greenland: one with realistic interannually varying runoff increasing in the early 2000s and the other with climatologically (1961–2000) continued runoff. The majority of the additional freshwater remains within the boundary current enhancing the density gradient towards the warm and salty interior waters yielding increased current velocities. The accelerated boundary current shows a tendency towards eddy shedding into the Labrador Sea interior. Further, the experiments allow to attribute higher stratification and shallower mixed layers southwest of Greenland and deeper mixed layers in the Irminger Sea, particularly in 2015–2018, to the runoff increase in the early 2000s.

## Plain Language Summary

Global warming has accelerated the melting of the Greenland ice sheet over the past few decades resulting in enhanced freshwater input into the North Atlantic. The additional freshwater can potentially inhibit deep water formation and have future implications on ocean circulation. To determine the impact from Greenland melt, we compare two high-resolution model experiments all with the same forcing but differing input of Greenland freshwater fluxes from 1997–2021. We find that in the experiment with realistically increasing Greenland meltwater, the water becomes fresher and cooler along the continental shelf and boundary of the subpolar gyre. The density difference between the shelf and interior increases with more freshwater, resulting in faster West Greenland Current speeds and enhanced eddy formation. Deeper mixed layers are found in the eastern Irminger Sea, particularly in 2015–2018. From 2009–2013, there were shallower mixed layers in the Labrador Sea where less Greenland meltwater was mixed downwards and spread eastward, causing mixed layers to deepen in the Irminger Sea.

## 1 Introduction

The Greenland ice sheet has been losing mass over the last couple of decades as a result of global warming (Hanna et al., 2008; Fettweis et al., 2011; Bamber et al., 2018). With an increasing amount of freshwater input, there has been interest in the impact it will have on circulation in the subpolar North Atlantic (SPNA), particularly whether additional freshwater will increase stratification and reduce deep water formation, which could weaken the Atlantic Meridional Overturning Circulation (AMOC) (Rahmstorf et al., 2015; Bakker et al., 2016; Böning et al., 2016; Swingedouw et al., 2022). Freshwater from Greenland melt will first appear in the East and West Greenland Currents (EGC/WGC) on top of Arctic sourced fresh Polar Water contained in these boundary currents (de Steur et al., 2009, 2018). Both the EGC and WGC consist of two surface intensified double current cores with a coastal current and outer slope current just beyond the shelfbreak (Bacon et al., 2002; Håvik et al., 2017; Sutherland & Pickart, 2008; Le Bras et al., 2018; Myers et al., 2009; Pacini et al., 2020; Gou et al., 2021). We will use the term boundary current to address both cores together as one system. The major current pathways are shown in Figure 1a.

The EGC is observed to be fairly coherent with minimal freshwater export along east Greenland; strong alongshore winds constrain the majority of fresh and cool water near the shelf (Sutherland & Pickart, 2008; Le Bras et al., 2018; Duyck et al., 2022; Schiller-Weiss et al., 2023). Along southeast Greenland at Cape Farewell, tip jets, northeasterly winds, and a retroflexion can export freshwater into the central Irminger Sea (Duyck et al., 2022; Holliday et al., 2007). The WGC consists of near surface buoyant and fresh

61 waters with warmer and salty Irminger water at depth (Gou et al., 2022; Myers et al.,  
 62 2007; Fratantoni & Pickart, 2007; Pacini et al., 2020). There are differing pathways fresh-  
 63 water is transported by the WGC, it can flow northward into Baffin Bay or cyclonically  
 64 around the Labrador basin (Pacini et al., 2021; Gou et al., 2021). Freshwater from the  
 65 WGC can be fluxed into the central Labrador Sea via offshore Ekman transport (Luo  
 66 et al., 2016; Castelao et al., 2019; Schulze Chretien & Frajka-Williams, 2018) and eddies  
 67 (Lilly et al., 2003; Katsman et al., 2004; Rieck et al., 2019; Pacini & Pickart, 2022). The  
 68 Labrador and Irminger Sea will both be referred to as LAB and IRM throughout the manuscript.

69 Eddies that are shed into the LAB from the boundary current have different ori-  
 70 gins. Irminger Rings are formed from steep topographic differences in the slope south  
 71 of Cape Desolation (CD) (Lilly et al., 2003; Bracco et al., 2008; Luo et al., 2011; de Jong  
 72 & de Steur, 2016; Rieck et al., 2019). Boundary current eddies are generated near the  
 73 shelf in the WGC and Labrador Current via baroclinic instabilities which intensify in  
 74 winter when currents strengthen (Katsman et al., 2004; Chanut et al., 2008; Rieck et al.,  
 75 2019). Eddies have been observed to play a significant role in determining the magni-  
 76 tude and location of deep convection, restratification, and preconditioning processes by  
 77 transporting heat and freshwater into the interior LAB and IRM (Gelderloos et al., 2011;  
 78 Chanut et al., 2008; Rieck et al., 2019). An eastward shift in deep convection was ob-  
 79 served from 2015–2018 (Zunino et al., 2020; Piron et al., 2017; Rhs et al., 2021), which  
 80 Rhs et al. (2021) hypothesized may partially be attributed to accelerated Greenland  
 81 melting. As more freshwater enters the boundary currents, it is important to understand  
 82 and identify associated hydrographic and potential dynamical changes.

83 In this study, we investigate the impact of Greenland freshwater input between two  
 84 nearly identical high-resolution, eddying ocean/sea-ice model runs from 1997–2021 but  
 85 with differing Greenland freshwater fluxes (FWFs). We break down the question for an  
 86 observable imprint by enhanced Greenland melting onto the ocean into the following subtopics:  
 87 (1) hydrographic changes i.e. in near-surface salinity and temperature (2) dynamical changes  
 88 i.e. changes in density and its influence on boundary current strength and eddy forma-  
 89 tion, and (3) changes in mixed layer depth (MLD) with a particular focus on additional  
 90 freshwater contributing to the eastward shift of deep convection.

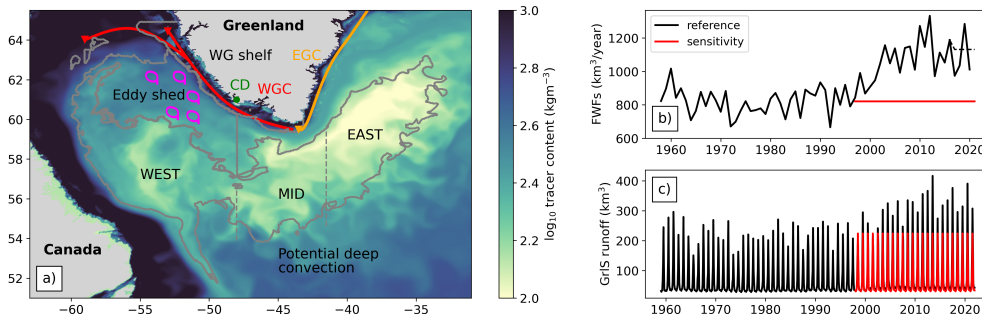


**Figure 1.** (a) Snapshot of passive tracer integrated over the top 200m and schematic of surface currents. The three gray contours show the West Greenland shelf, eddy shedding region (eddies marked by fuchsia rings), and the area of potential deep convection split into three sub-regions: LAB (WEST), south of Cape Farewell (MID), and IRM (EAST). Cape Desolation (CD) location marked in green. (b) Total, annual FWFs from Greenland runoff from 1960–2021. (c) Monthly varying FWFs. Black line shows interannually varying FWF of REF, dashed line shows 2012–2016 mean; the red line shows the reduced, climatological FWF from SENS.

## 2 Ocean Model Experiments

We compare two nearly identical model simulations from the ocean/sea-ice general circulation model configuration VIKING20X (Biastoch et al., 2021) (model details described in Supporting Information): one including the observed increase in Greenland runoff (hereafter referred to as "reference", short REF) and a "sensitivity" experiment (SENS), where the Greenland FWFs is reduced to the climatology of 1961–2000. In REF Greenland FWFs are interannually varying with an increasing trend shown in the total annual FWFs (black line of Figure 1b), based on (Bamber et al., 2018; Slater et al., 2021). The FWFs are monthly varying with a prominent seasonal cycle (Figure 1c) and are released at the surface and coastline, tagged by an accumulated passive tracer (Figure 1a). Greenland FWFs from Bamber et al. (2018) do not extend beyond 2016 and runoff in the JRA55-do forcing data set is continued by maintaining a daily varying climatology of 2012–2016 (Tsujino et al., 2018). In order to include a fair representation of the years after 2016, in particular the record runoff year 2019 (Tedesco & Fettweis, 2020), we computed a scaling factor for the JRA55-do Greenland runoff after 2016 based on the study of Slater et al. (2021), which provides satellite-derived measurements of Greenland runoff variability. While the scaling is based on the total Greenland runoff, the factor is applied to local FWFs per model grid cell to generate the forcing, i.e. the spatial pattern of the Greenland FWF is still tied to the 2012–2016 mean. SENS differs from the reference run in Greenland FWFs here represented as daily climatology from 1961–2000 (red line representing the suppressed FWFs in Figure 1b, c).

## 3 Results

The following analysis focuses on significant changes between REF and SENS. We first start by investigating significant sea surface salinity (SSS) and temperature (SST) differences, then changes in the West Greenland boundary current strength, followed by differences in eddy kinetic energy (EKE) to investigate the potential for enhanced eddy formation from changes in the boundary current. Lastly we attribute a deepening of mixed layers in the IRM to the enhanced FWF in REF (particularly in 2015–2018) and discuss the mechanisms leading to a contribution by Greenland meltwater to the eastward shift of deep convection in recent years.

### 3.1 Surface freshening and cooling

The first imprint of enhanced Greenland FWFs in the hydrography appears along the Greenland shelf. We focus on the last 20 years of the simulation (2002 - 2021) to allow for the additional freshwater to quasi-equilibrate (the linear trend in total Greenland FWF applied to REF is nearly zero over these two decades). We focus on annual means and compute differences (REF minus SENS) showing a significant freshening and cooling in SSS and SST particularly along the continental shelves (Figure 2a, b). Freshening and cooling appear throughout the year, with fresher water near the shelf in summer clearly associated with the seasonal peak in Greenland runoff (Bamber et al., 2018) (Figure S1a, c).

Significant areas of the SSS difference, purple in Figure 2a implying lower salinities in REF compared to SENS, are found primarily in the WGC, the LAB shelf, and eddy shedding region. We define the WGC boundaries by the 1000 m isobath and the eddy shedding boundary between the 1000 and 2000 m isobath (Figure 1a). The southern boundary is limited by the potential deep convection area (pDCA), defined as any grid point where MLDs exceed  $z_{critical} = 1000$  m at least once (Rühs et al., 2021) between 2002–2021 (Figure 1a). Statistical significance is computed from bootstrap resampling (Bertino et al., 2003) where significant areas are defined when the difference between the resampled means are larger than the total standard deviation of the two bootstrapped runs.

141 The coolest SSTs occur near the shelves and eddy shedding region where the LAB's  
142 shelf boundary exhibits anomalously cooler SSTs in REF (Figure 2b). The strong cool-  
143 ing around the northwest LAB boundary is associated with a greater extent of winter  
144 sea ice in REF (Figure S1a, c, e) attributed to local sea-ice formation and export from  
145 Baffin Bay (Våge et al., 2009; Kwok, 2007). (Deser et al., 2002) also observed that sea  
146 ice formation lagged changes in salinity along the WGC by 8 months i.e. summer melt-  
147 ing affects the LAB's northern sea ice extent.

148 2010 and 2012 were two years of exceptional Greenland runoff (Tedesco et al., 2011;  
149 Hanna et al., 2014) (Figure 1b). This is most evident in the WGC where both REF and  
150 SENS decrease in salinity from 2010–2012 (Figure 2c). Although 2019 was a year of anoma-  
151 lous Greenland melt, the majority of melt occurred further northwest of the ice sheet  
152 (Tedesco & Fettweis, 2020), thus the salinity decrease is less than in 2010 and 2012. 2012  
153 remaining the year of strongest Greenland melt on record from higher humidity and air  
154 temperature over the ice sheet (Tedesco & Fettweis, 2020).

155 REF has lower annual mean salinities than SENS in the WGC where the salini-  
156 ties show a larger spread between the two runs beginning in 2004, a few years after the  
157 rapid increase in Greenland FWFs from 2000 onwards (Figure 1b). The eddy shedding  
158 region exhibits less of a spread in SSS annual means than found in the WGC. Interest-  
159 ingly, the strong reduction in SSS begins in 2011 rather than 2010, a year with record  
160 runoff. Alongshore winds were downwelling favorable in the winter of 2010 following the  
161 exceptional summer runoff and hence offshore transport of relatively fresh waters was  
162 even less than in 2011 (Figure S2) (Myers et al., 2021), highlighting the importance of  
163 wind forcing over runoff for freshening events offshore the WGC.

164 The VIKING20X-JRA OMIP hindcast run from which both REF and SENS are  
165 branched off in 1997, shows quasi multi-decadal variability with lower salinities in the  
166 1970s and 2000s and higher salinities in the 1980s–1990s. The sharp decrease in salin-  
167 ity in both the WGC and eddy shedding region in 1969 is identified as the Great Salin-  
168 ity anomaly from 1968–1982 (GSA'70s) resulting from anomalous Arctic export via Fram  
169 Strait (Dickson et al., 1988; Belkin et al., 1998). In REF, the period of 2010–2012 at-  
170 tributed to exceptional Greenland runoff reaches even lower SSS values than the GSA'70s  
171 emphasizing the significance that Greenland FWFs has on the boundary current.

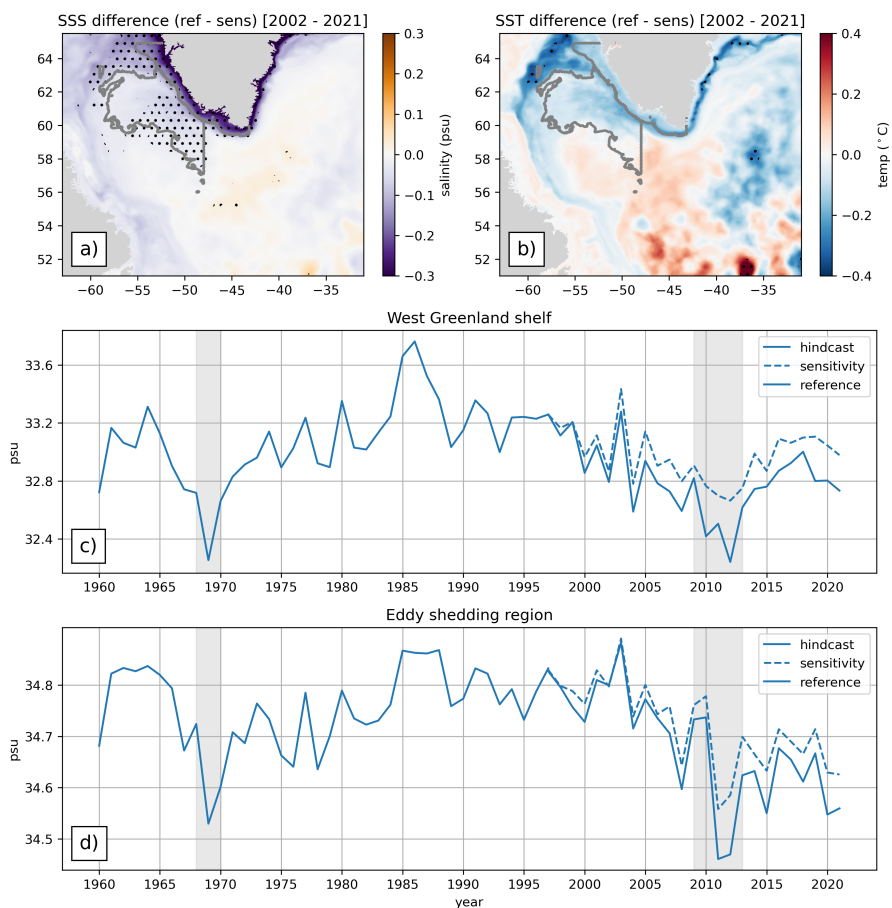


**Figure 2.** (a) Mean surface salinity (2002–2021) response (REF minus SENS) and (b) mean sea surface temperature difference. Black stippling indicating significant areas. Gray contours mark the West Greenland shelf and eddy shedding region. (c) Annual mean SSS over the West Greenland shelf. (d) Annual mean SSS over the eddy shedding region. The solid line is based on the hindcast simulation (1960–1996) and from REF in 1997–2021; the dashed line represents SENS. Gray vertical bars indicate the GSA’70s and 2010–2012 years of strong Greenland melt.

172

### 3.2 Strengthened boundary current

173

174

175

176

177

178

179

180

181

182

183

184

185

186

The enhanced Greenland runoff over the recent decades contributes to the fresh polar watermass carried by the Greenland boundary current system—with the shown near-surface cooling contributing a slight but less effective density offset (Figure S1e, f). The density decrease on the shelf intensifies the horizontal gradient towards the denser interior LAB and strengthens the WGC via thermal wind balance (Gou et al., 2022; Katsman et al., 2004). To investigate these changes in the boundary current system, we take an exemplary cross section at OSNAP West (Lozier et al., 2019) to obtain the velocity structure of the WGC in REF (Figure 3a). The boundary current consists of two current cores both reaching velocity magnitudes up to 0.5 m/s: the West Greenland coastal current (WGCC) and just off the shelfbreak, the slope current. The WGCC contains the most polar water along with traces of Greenland meltwater (Lin et al., 2018; Pacini et al., 2020; Gou et al., 2022). The slope current is adjacent and lies above the saltier and warmer Irminger Current (Fratantoni & Pickart, 2007; Myers et al., 2009). We isolate the surface intensified WGCC and slope current by taking the top 100 m and northwest-

187 ward velocities only (black boxes in Figure 3a). We sample the WGC system by select-  
 188 ing only the top 100 m as a conservative choice to focus on the fresh and fast WGC (Gou  
 189 et al., 2021).

190 The slope current (Figure 3b, orange lines) has greater annual mean velocities from  
 191 2002–2021 on average than the WGCC (blue lines) and appears to increase while the WGCC  
 192 shows stronger interannual variability. At OSNAP West, slope current speed has an in-  
 193 creasing trend over the last two decades, also found by (Gou et al., 2022) south of Fylla  
 194 Bank. Both the mean WGCC and slope current velocities are greater in REF (solid lines)  
 195 than in SENS, particularly in 2011 where the speeds deviate more (Figure 3b). While  
 196 the increase in REF is relatively small, the bootstrapped means are statistically signifi-  
 197 cant where the resampled reference mean velocity for both currents are greater than the  
 198 90<sup>th</sup> percentile of the resampled SENS velocities. As the spread increases towards 2021,  
 199 we speculate that this signal will emerge more clearly over the next years. Note that in  
 200 contrast to earlier hosing and freshwater-release experiments, the much smaller observed  
 201 increase in Greenland FWF studied here can only drive a slight increase in the bound-  
 202 ary current speed.

203 Nevertheless, at OSNAP West there is a significantly faster flow speed increasing  
 204 the potential for local instabilities causing more eddies to be shed into the interior (Gou  
 205 et al., 2023; Chanut et al., 2008; Katsman et al., 2004). We thus analyze the EKE af-  
 206 ter discussing the thermal wind balance effect. The surface density gradient between the  
 207 shelf and interior increases due to enhanced runoff, resulting in a faster boundary cur-  
 208 rent. To investigate this, we evaluate a “cumulative correlation” formed by the sum of  
 209 the Pearson’s correlation coefficient (capped at 1.0) between the WGCC and slope cur-  
 210 rent mean speed at OSNAP West, CD, and Fylla Bank and the horizontal density gra-  
 211 dient at the surface in REF (Figure 3c, d). The current structure and correlation map  
 212 per cross section are discussed further in Supporting Information Text and Figure S3.

213 The WGCC shows a band of higher positive cumulative correlations surrounding  
 214 the Greenland coast (Figure 3c), which illustrates the strong link between a strength-  
 215 ening of the current speed and an increase in the density gradient across the shelf break.  
 216 In addition to the strengthening of the density gradient, the dipole pattern created by  
 217 a band of negative correlations just offshore, suggests an inshore movement of the sharp  
 218 density gradient following the shelf break in periods with intensified WGCC flow speeds.  
 219 In contrast, the cumulative correlation between the slope current and the density gra-  
 220 dient shows a less confined pattern (Figure 3d), where a patch of positive cumulative cor-  
 221 relations is found in the northeast LAB and the eddy shedding region.

222 We argue that the greater area of positive correlations with the slope current is driven  
 223 by an enhanced eddy activity during increased flow speed along the shelf slope. Since  
 224 horizontal density gradients are computed per model grid cell, the sharp fronts of mesoscale  
 225 eddies dominate an area of otherwise smaller horizontal density fluctuations. The rel-  
 226 atively strong correlation with the accelerating slope current (Figures 3b, d) hints at grow-  
 227 ing eddy activity in this region. Does this mean that EKE is enhanced in REF over SENS,  
 228 i.e. is there a change in eddy activity related to enhanced Greenland FWFs?

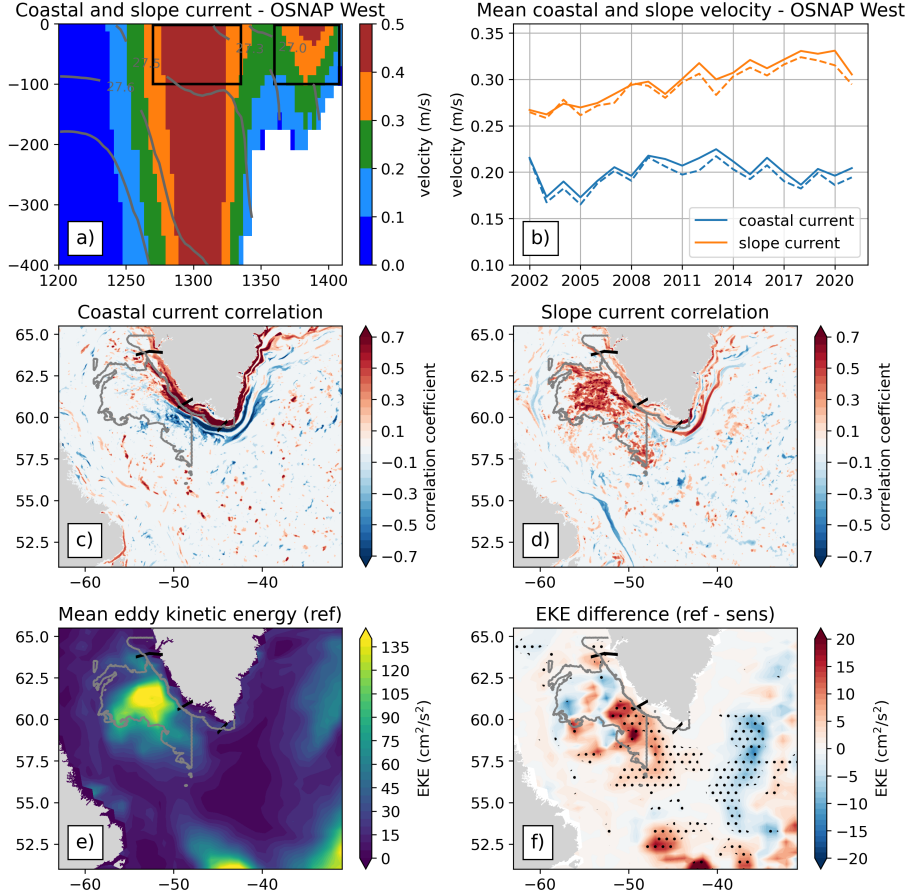


**Figure 3.** (a) Mean (2002–2021) current velocity magnitude at OSNAP West. Black boxes show the coastal and slope current cores. (b) Annual mean coastal (blue) and slope current (orange) velocity time series. Dashed/solid is the SENS/REF. (c) Cumulative correlation between the surface horizontal density gradient and WGCC at OSNAP West, CD, and Fylla Bank (south to north cross sections in black lines). (d) Cumulative correlation at the slope current. (e) The mean EKE at 100m depth from the REF. (f) Mean EKE difference (REF minus SENS). Stippling indicates the significant areas.

229 In both experiments, the majority of eddies are formed in the northeast corner of  
 230 the LAB, just off of CD, marked in Figure 1a), from large topographic changes which  
 231 generate Irminger Rings (Bracco et al., 2008), shown by the patch of high EKE (Figure  
 232 3e). As the eddy field is highly variable, we coarsen the EKE field to  $\approx 1/4^\circ$  for smooth-  
 233 ing. When computing the mean EKE difference between the REF and SENS (Figure 3f),  
 234 we find significant positive EKE differences just southwest of OSNAP West where lower  
 235 salinities leak into the interior (Figure 2a). The positive difference does not extend over  
 236 the whole eddy shedding region, particularly where the EKE is greatest just north of CD.  
 237 Gou et al. (2021) observed that the WGCC splits into multiple branches at Juliannehaab  
 238 Bight but merges again at CD. Boundary current eddies are induced from baroclinic in-  
 239 stabilities as the WGC meanders (Pacini & Pickart, 2022), which may explain the posi-  
 240 tive EKE difference where the local density gradient between the fresh (and cool) bound-  
 241 ary current and saltier interior from increased runoff. This likely causes baroclinic in-  
 242 stabilities to form or strengthen resulting in more eddies. However, such eddies are typi-  
 243 cally smaller and shallower than eddies shed at CD from local topography (Pacini & Pickart,

244 2022). This could explain for differences in EKE between REF and SENS to not be sig-  
 245 nificant (stippling in Figure 3f). Another reason is the large internal variability of mesoscale  
 246 dynamics in this region in both simulations.

247 Enhanced EKE southwest of Greenland in REF indicates a role for eddies in the  
 248 near-surface freshening (and cooling) in this region being all triggered by increased Green-  
 249 land FWFs and having implications for preconditioning of and restratification after deep  
 250 convection (Gelderloos et al., 2011; Chanut et al., 2008).

### 251 3.3 Eastward deepening of mixed layer depth

252 We investigate the changes in MLD between the experiments to identify a poten-  
 253 tial impact by enhanced Greenland FWFs over the recent two decades. Deep convection  
 254 typically occurs yearly in the LAB but differs in strength (Yashayaev & Clarke, 2008;  
 255 Zunino et al., 2020). There have been periods of deep convective activity occurring in  
 256 the IRM, particularly in 2009, 2012, and 2015–2018 from favorable preconditioning the  
 257 preceding years (Zunino et al., 2020; de Jong & de Steur, 2016; Piron et al., 2016; Yashayaev  
 258 & Loder, 2017; Piron et al., 2017; Rühls et al., 2021). Labrador Sea Water (LSW) is formed  
 259 at mid-depth (500–2000m) during convection and can spread eastward into the IRM on  
 260 time scales of 1–3 years (Lavender et al., 2000; Straneo et al., 2003; Yashayaev et al., 2007;  
 261 Chafik et al., 2022; Böning et al., 2023). Rühls et al. (2021) speculated that freshening  
 262 trends in the SPNA may have resulted in this intensified deep convection in the IRM from  
 263 2015–2018. While it is observed that changes in MLD are dominated by winter air-sea  
 264 heat fluxes versus changes in stratification (de Jong et al., 2012; de Jong & de Steur, 2016;  
 265 Piron et al., 2017), the question remains whether traces of Greenland melt may have par-  
 266 tially contributed to the deepening of mixed layers in the east. Note, the atmospheric  
 267 forcing is the same for REF and SENS and hence surface fluxes are virtually equal thus  
 268 allowing attribution of MLD differences between REF and SENS to the enhanced Green-  
 269 land runoff.

270 We focus on the years 2009–2013, just prior to the period of strong deep convec-  
 271 tion, and 2015–2018. The long term mean (2002–2021) shows deepest MLDs primarily  
 272 in the central LAB (Figure 4a). In 2009–2013 deep convection was confined to the LAB  
 273 (pink contour in 4a, b), while 2009 and 2012 were individual years where the MLDs reached  
 274 depths greater than 1500m in the LAB and  $\approx$ 1000m south of Cape Farewell (MID, cf.  
 275 Figure 1a) (Figure S4a, b).

276 Deep convection occurred in both the LAB and IRM (black contour in Figure 4a,  
 277 b) in 2015–2018. When computing the maximum MLD difference (REF minus SENS)  
 278 from 2015–2018, we find significantly deeper MLDs in the IRM in REF than in SENS,  
 279 with differences ranging from 200–600 m (Figure 4b). This is seen in the convective re-  
 280 sistance (CR), defined by the amount of vertical integral buoyancy anomaly that must  
 281 be removed in order to overcome stratification and mix down to a particular depth ( $h=1500$ m)  
 282 (Gillard et al., 2022; Frajka-Williams et al., 2014; Holdsworth & Myers, 2015) (Support-  
 283 ing Information S5). Shallower MLDs dominate the LAB in REF, particularly between  
 284 WEST and MID (Figure 4b), coinciding with significant, higher CRs in REF in the LAB  
 285 (Figure S5b).

286 To investigate whether Greenland melting has contributed to an eastward deep-  
 287 ening of MLDs in 2015–2018, we look at winter mean depth profiles averaged along the  
 288 pDCA over maximum band of  $\pm 5^\circ$  latitude from 2009–2013. Stratification increases up  
 289 to 20% in REF with respect to SENS in the LAB (WEST) below 300 m (Figure 4c).

290 Stratification difference between REF and SENS in the IRM (EAST) shows a promi-  
 291 nent dipole with reduced stratification in REF up to 30% above 1000–1500 m and greater  
 292 stratification below. There is an outstanding reduction in passive meltwater tracer con-  
 293 centration in EAST in REF compared to SENS below the same depth interface contoured

294 by said stratification response dipole (red patch in Figure 4d), i.e. aligned with the stronger  
 295 stratification in REF. Tracer content is enhanced above this 1000–1500 m interface match-  
 296 ing the weaker stratification. For WEST and MID, the cross-section shows enhanced tracer  
 297 content over the entire column which is expected since FWFs in REF are larger than  
 298 in SENS. Together, these patterns hint at freshwater being convected to greater depth  
 299 in the LAB in SENS prior to being exported to EAST with the LSW (deeper LAB MLDs  
 300 in SENS in Figure 4c, d). Since we are averaging over 5 years, there is a smoothing over  
 301 the annual maximum MLDs, where the MLD discrepancy between REF and SENS is  
 302 strongest in 2009 and 2012 (Figure S4a, c).

303 We interpret these signals such that firstly, enhanced Greenland FWFs cause re-  
 304 duced deep mixing in the LAB, leading to meltwater being entrained at a shallower depth  
 305 before being exported to the IRM. Secondly, the meltwater now residing between 200–  
 306 1000 m (instead of further down) acts to decrease stratification between mid-depth and  
 307 the surface, also illustrated by a reduced CR in EAST in REF versus SENS (Figure S5c,  
 308 green line). As a result, the water column in the central to eastern IRM was precondi-  
 309 tioned for deeper mixing prior to the occurrence of favorable atmospheric conditions trig-  
 310 gering convection in 2015 and following years. A shift in deep convection center from the  
 311 LAB to the IRM under enhanced freshwater input from Greenland appears to be a com-  
 312 mon response among coupled climate models (e.g., Devilliers et al., 2021; Martin et al.,  
 313 2022; Martin & Biastoch, 2023).

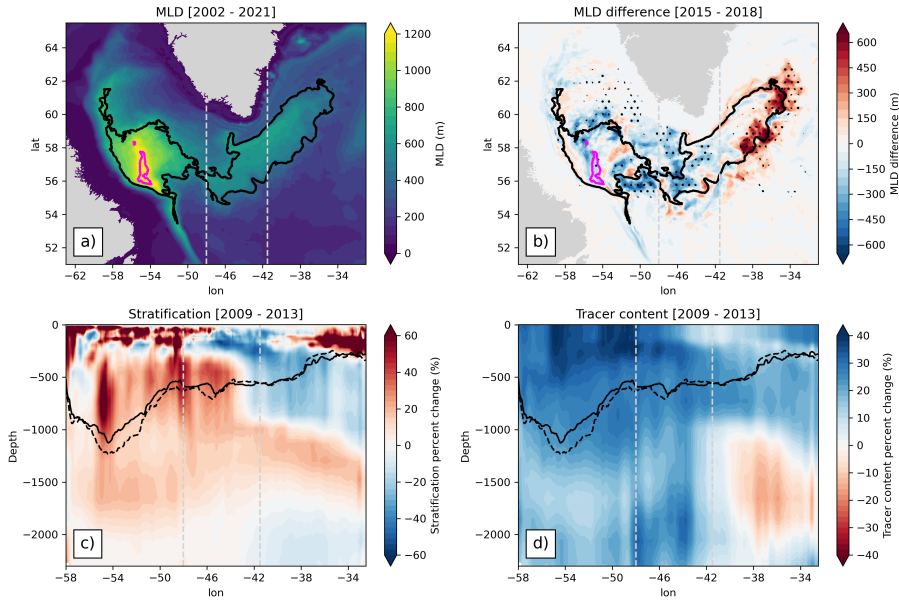


**Figure 4.** (a) The maximum 2002–2021 mean MLD (REF). (b) The MLD difference (REF minus SENS) in 2015–2018. Stippling indicates significant areas, the pink/black contour shows the deep convection area in 2009–2013/2015–2018. (c) The winter mean (2008–2013) stratification percent change of REF compared to SENS averaged over the pDCA. (d) The Greenland tracer content percent change. Black solid/dashed line indicates the mean maximum MLD of the REF/SENS. The gray dashed, vertical lines indicate the WEST/MID/EAST separations.

314 Thus, we suggest that preconditioning of the IRM at mid-depth began in 2009–2013  
 315 when the LAB’s MLDs exceeded  $z_{critical}$  allowing for deep entrainment of meltwater. This  
 316 process preceded the propagation of fresher waters into the IRM in 2017–2018 (Biló et

al., 2022) originating from the Eastern North Atlantic salinity anomaly of 2012–2016 (Holliday et al., 2020). It is noteworthy that the comparatively small but realistic increase in FWFs in REF helped reduce CR to as low as  $0.2 \text{ m}^2/\text{s}^2$  in EAST, which was not the case for EAST since the GSA in the late 1980s, e.g. the minimum CR in WEST was twice as strong in recent years as during the 1990s (Figure S5c). We highlight that: 1) enhanced runoff of Greenland meltwater is not vertically mixed as deep from greater/reduced CRs/MLDs in the LAB, 2) stratification in the IRM decreases upon more freshwater entering the upper 1000 m enabling deeper MLDs there, and 3) increasing Greenland FWFs reduces the IRM’s CR after 2009 reaching even lower levels than the LAB.

## 4 Conclusions

In this study we analyze two  $1/20^\circ$  ocean/sea-ice model simulations with the same surface forcing except for Greenland freshwater input: REF containing realistically varying FWFs, and SENS with reduced FWFs based on a climatological mean (1961–2000). We conclude that while there has not yet been a significant impact by accelerated Greenland melting on large scale circulation, the most notable emerging imprints are:

1) The boundary current shows the largest signal in hydrographic changes. There is a significant freshening around the WGC system which intrudes into the eddy shedding region, reducing the density on and near the shelf. Cooler temperatures dominate the boundary currents, with enhanced sea ice coverage in the northwest perimeter of the Labrador basin.

2) The shelf’s reduced density increases the density gradient between the slope current and interior Labrador/Irminger seas, where the coastal and slope currents strengthen i.e. at OSNAP West. The increase in density gradients and current strength can result in barotropic and baroclinic instabilities leading to intensified eddy shedding. The increased eddy activity southwest of Greenland favors an enhanced “leaking” of meltwater into the Labrador Sea.

3) The intrusion of relatively fresher waters into the deep convection region reduces—but does not prohibit—deep mixing in the Labrador Sea. The signal is entrained to shallower depths only and is exported into the Irminger Sea via LSW, reducing stratification between the surface and mid-depth. We argue that our experiment demonstrates that by this process, enhanced Greenland runoff has contributed to a lowering of convective resistance in the Irminger Sea and an eastward shift of deep convection in 2015–2018.

## Data Availability Statement

All (processed) model data and scripts needed for Figures 1–4 are made available using the GEOMAR data management platform under the identifier: [hdl.handle.net/20.500.12085/e3cd8f8c-07bd-4955-b77a-504377e299ac](https://hdl.handle.net/20.500.12085/e3cd8f8c-07bd-4955-b77a-504377e299ac) (Schiller-Weiss et al., 2024).

## Acknowledgments

This work was carried out in the G-Shocx project (MA 4039/1-1) supported by the Deutsche Forschungsgemeinschaft (DFG). The authors thank Willi Rath and Tobias Schulzki for technical and scientific support.

## References

Bacon, S., Reverdin, G., Rigor, I. G., & Snaith, H. M. (2002). A freshwater jet on the east Greenland shelf. *Journal of Geophysical Research: Oceans*, *107*(C7),

- 361 5–1–5–16. doi: 10.1029/2001JC000935
- 362 Bakker, P., Schmittner, A., Lenaerts, J. T. M., Abe-Ouchi, A., Bi, D., van den  
363 Broeke, M. R., . . . Yin, J. (2016). Fate of the Atlantic Meridional Over-  
364 turning Circulation: Strong decline under continued warming and Green-  
365 land melting. *Geophysical Research Letters*, *43*(23), 12,252–12,260. doi:  
366 10.1002/2016GL070457
- 367 Bamber, J. L., Tedstone, A. J., King, M. D., Howat, I. M., Enderlin, E. M., van den  
368 Broeke, M. R., & Noel, B. (2018). Land Ice Freshwater Budget of the Arctic  
369 and North Atlantic Oceans: 1. Data, Methods, and Results. *Journal of Geo-*  
370 *physical Research: Oceans*, *123*(3), 1827–1837. doi: 10.1002/2017JC013605
- 371 Belkin, I. M., Levitus, S., Antonov, J., & Malmberg, S.-A. (1998, January). “Great  
372 Salinity Anomalies” in the North Atlantic. *Progress in Oceanography*, *41*(1),  
373 1–68. doi: 10.1016/S0079-6611(98)00015-9
- 374 Bertino, L., Evensen, G., & Wackernagel, H. (2003). Sequential Data Assimilation  
375 Techniques in Oceanography. *International Statistical Review*, *71*(2), 223–241.  
376 doi: 10.1111/j.1751-5823.2003.tb00194.x
- 377 Biastoch, A., Schwarzkopf, F. U., Getzlaff, K., Rühls, S., Martin, T., Scheinert, M.,  
378 . . . Böning, C. W. (2021, September). Regional imprints of changes in the  
379 Atlantic Meridional Overturning Circulation in the eddy-rich ocean model  
380 VIKING20X. *Ocean Science*, *17*(5), 1177–1211. doi: 10.5194/os-17-1177-2021
- 381 Biló, T. C., Straneo, F., Holte, J., & Le Bras, I. a.-A. (2022). Arrival of New Great  
382 Salinity Anomaly Weakens Convection in the Irminger Sea. *Geophysical Re-*  
383 *search Letters*, *49*(11), e2022GL098857. doi: 10.1029/2022GL098857
- 384 Bracco, A., Pedlosky, J., & Pickart, R. S. (2008, September). Eddy Formation near  
385 the West Coast of Greenland. *Journal of Physical Oceanography*, *38*(9), 1992–  
386 2002. doi: 10.1175/2008JPO3669.1
- 387 Böning, C. W., Behrens, E., Biastoch, A., Getzlaff, K., & Bamber, J. L. (2016,  
388 July). Emerging impact of Greenland meltwater on deepwater formation  
389 in the North Atlantic Ocean. *Nature Geoscience*, *9*(7), 523–527. doi:  
390 10.1038/ngeo2740
- 391 Böning, C. W., Wagner, P., Handmann, P., Schwarzkopf, F. U., Getzlaff, K., & Bi-  
392 astoch, A. (2023, August). Decadal changes in Atlantic overturning due to  
393 the excessive 1990s Labrador Sea convection. *Nature Communications*, *14*(1),  
394 4635. doi: 10.1038/s41467-023-40323-9
- 395 Castelao, R. M., Luo, H., Oliver, H., Rennermalm, A. K., Tedesco, M., Bracco, A.,  
396 . . . Medeiros, P. M. (2019). Controls on the Transport of Meltwater From  
397 the Southern Greenland Ice Sheet in the Labrador Sea. *Journal of Geophysical*  
398 *Research: Oceans*, *124*(6), 3551–3560. doi: 10.1029/2019JC015159
- 399 Chafik, L., Holliday, N. P., Bacon, S., & Rossby, T. (2022). Irminger Sea Is the Cen-  
400 ter of Action for Subpolar AMOC Variability. *Geophysical Research Letters*,  
401 *49*(17), e2022GL099133. doi: 10.1029/2022GL099133
- 402 Chanut, J., Barnier, B., Large, W., Debreu, L., Penduff, T., Molines, J. M., & Math-  
403 iot, P. (2008, August). Mesoscale Eddies in the Labrador Sea and Their  
404 Contribution to Convection and Restratification. *Journal of Physical Oceanog-*  
405 *raphy*, *38*(8), 1617–1643. doi: 10.1175/2008JPO3485.1
- 406 de Jong, M. F., & de Steur, L. (2016). Strong winter cooling over the Irminger  
407 Sea in winter 2014–2015, exceptional deep convection, and the emergence of  
408 anomalously low SST. *Geophysical Research Letters*, *43*(13), 7106–7113. doi:  
409 10.1002/2016GL069596
- 410 de Jong, M. F., van Aken, H. M., Våge, K., & Pickart, R. S. (2012, May). Convec-  
411 tive mixing in the central Irminger Sea: 2002–2010. *Deep Sea Research Part I:*  
412 *Oceanographic Research Papers*, *63*, 36–51. doi: 10.1016/j.dsr.2012.01.003
- 413 Deser, C., Holland, M., Reverdin, G., & Timlin, M. (2002). Decadal varia-  
414 tions in Labrador Sea ice cover and North Atlantic sea surface tempera-  
415 tures. *Journal of Geophysical Research: Oceans*, *107*(C5), 3–1–3–12. doi:

- 416 10.1029/2000JC000683  
 417 de Steur, L., Hansen, E., Gerdes, R., Karcher, M., Fahrbach, E., & Holfort, J.  
 418 (2009). Freshwater fluxes in the East Greenland Current: A decade of ob-  
 419 servations. *Geophysical Research Letters*, *36*(23). doi: 10.1029/2009GL041278  
 420 de Steur, L., Peralta-Ferriz, C., & Pavlova, O. (2018). Freshwater Ex-  
 421 port in the East Greenland Current Freshens the North Atlantic.  
 422 *Geophysical Research Letters*, *45*(24), 13,359–13,366. (eprint:  
 423 <https://onlinelibrary.wiley.com/doi/pdf/10.1029/2018GL080207>) doi:  
 424 10.1029/2018GL080207  
 425 Devilliers, M., Swingedouw, D., Mignot, J., Deshayes, J., Garric, G., & Ayache, M.  
 426 (2021, November). A realistic Greenland ice sheet and surrounding glaciers  
 427 and ice caps melting in a coupled climate model. *Climate Dynamics*, *57*(9),  
 428 2467–2489. doi: 10.1007/s00382-021-05816-7  
 429 Dickson, R. R., Meincke, J., Malmberg, S.-A., & Lee, A. J. (1988, January). The  
 430 “great salinity anomaly” in the Northern North Atlantic 1968–1982. *Progress*  
 431 *in Oceanography*, *20*(2), 103–151. doi: 10.1016/0079-6611(88)90049-3  
 432 Duyck, E., Gelderloos, R., & de Jong, M. F. (2022). Wind-Driven Freshwater Ex-  
 433 port at Cape Farewell. *Journal of Geophysical Research: Oceans*, *127*(5),  
 434 e2021JC018309. doi: 10.1029/2021JC018309  
 435 Fettweis, X., Tedesco, M., van den Broeke, M., & Ettema, J. (2011, May). Melting  
 436 trends over the Greenland ice sheet (1958–2009) from spaceborne microwave  
 437 data and regional climate models. *The Cryosphere*, *5*(2), 359–375. doi:  
 438 10.5194/tc-5-359-2011  
 439 Frajka-Williams, E., Rhines, P. B., & Eriksen, C. C. (2014, January). Horizontal  
 440 Stratification during Deep Convection in the Labrador Sea. *Journal of Physical*  
 441 *Oceanography*, *44*(1), 220–228. doi: 10.1175/JPO-D-13-069.1  
 442 Fratantoni, P. S., & Pickart, R. S. (2007, October). The Western North Atlantic  
 443 Shelfbreak Current System in Summer. *Journal of Physical Oceanography*,  
 444 *37*(10), 2509–2533. doi: 10.1175/JPO3123.1  
 445 Gelderloos, R., Katsman, C. A., & Drijfhout, S. S. (2011, November). Assess-  
 446 ing the Roles of Three Eddy Types in Restratifying the Labrador Sea after  
 447 Deep Convection. *Journal of Physical Oceanography*, *41*(11), 2102–2119. doi:  
 448 10.1175/JPO-D-11-054.1  
 449 Gillard, L. C., Pennelly, C., Johnson, H. L., & Myers, P. G. (2022, March).  
 450 The Effects of Atmospheric and Lateral Buoyancy Fluxes on Labrador  
 451 Sea Mixed Layer Depth. *Ocean Modelling*, *171*, 101974. doi: 10.1016/  
 452 j.ocemod.2022.101974  
 453 Gou, R., Feucher, C., Pennelly, C., & Myers, P. G. (2021). Seasonal cycle of the  
 454 coastal west greenland current system between cape farewell and cape deso-  
 455 lation from a very high-resolution numerical model. *Journal of Geophysical*  
 456 *Research: Oceans*, *126*(5), e2020JC017017. doi: [https://doi.org/10.1029/](https://doi.org/10.1029/2020JC017017)  
 457 [2020JC017017](https://doi.org/10.1029/2020JC017017)  
 458 Gou, R., Li, P., Wiegand, K. N., Pennelly, C., Kieke, D., & Myers, P. G. (2023,  
 459 October). Variability of Eddy Formation off the West Greenland Coast from  
 460 a 1/60° Model. *Journal of Physical Oceanography*, *53*(10), 2475–2490. doi:  
 461 10.1175/JPO-D-23-0004.1  
 462 Gou, R., Pennelly, C., & Myers, P. G. (2022). The Changing Behavior of  
 463 the West Greenland Current System in a Very High-Resolution Model.  
 464 *Journal of Geophysical Research: Oceans*, *127*(8), e2022JC018404. doi:  
 465 10.1029/2022JC018404  
 466 Hanna, E., Fettweis, X., Mernild, S. H., Cappelen, J., Ribergaard, M. H., Shuman,  
 467 C. A., ... Mote, T. L. (2014). Atmospheric and oceanic climate forcing of the  
 468 exceptional Greenland ice sheet surface melt in summer 2012. *International*  
 469 *Journal of Climatology*, *34*(4), 1022–1037. doi: 10.1002/joc.3743  
 470 Hanna, E., Huybrechts, P., Steffen, K., Cappelen, J., Huff, R., Shuman, C., ... Grif-

- 471 fiths, M. (2008, January). Increased Runoff from Melt from the Greenland Ice  
 472 Sheet: A Response to Global Warming. *Journal of Climate*, *21*(2), 331–341.  
 473 doi: 10.1175/2007JCLI1964.1
- 474 Holdsworth, A. M., & Myers, P. G. (2015, June). The Influence of High-Frequency  
 475 Atmospheric Forcing on the Circulation and Deep Convection of the Labrador  
 476 Sea. *Journal of Climate*, *28*(12), 4980–4996. doi: 10.1175/JCLI-D-14-00564.1
- 477 Holliday, N. P., Bersch, M., Berx, B., Chafik, L., Cunningham, S., Florindo-López,  
 478 C., ... Yashayaev, I. (2020, January). Ocean circulation causes the largest  
 479 freshening event for 120 years in eastern subpolar North Atlantic. *Nature*  
 480 *Communications*, *11*(1), 585. doi: 10.1038/s41467-020-14474-y
- 481 Holliday, N. P., Meyer, A., Bacon, S., Alderson, S. G., & de Cuevas, B. (2007).  
 482 Retroreflection of part of the east Greenland current at Cape Farewell. *Geophys-*  
 483 *ical Research Letters*, *34*(7). doi: 10.1029/2006GL029085
- 484 Håvik, L., Pickart, R. S., Våge, K., Torres, D., Thurnherr, A. M., Beszczynska-  
 485 Möller, A., ... von Appen, W.-J. (2017). Evolution of the East Greenland  
 486 Current from Fram Strait to Denmark Strait: Synoptic measurements from  
 487 summer 2012. *Journal of Geophysical Research: Oceans*, *122*(3), 1974–1994.  
 488 doi: 10.1002/2016JC012228
- 489 Katsman, C. A., Spall, M. A., & Pickart, R. S. (2004, September). Boundary Cur-  
 490 rent Eddies and Their Role in the Restratification of the Labrador Sea. *Jour-*  
 491 *nal of Physical Oceanography*, *34*(9), 1967–1983. doi: 10.1175/1520-0485(2004)  
 492 034<1967:BCEATR>2.0.CO;2
- 493 Kwok, R. (2007). Baffin Bay ice drift and export: 2002–2007. *Geophysical Research*  
 494 *Letters*, *34*(19). doi: 10.1029/2007GL031204
- 495 Lavender, K. L., Davis, R. E., & Owens, W. B. (2000, September). Mid-depth recir-  
 496 culation observed in the interior Labrador and Irminger seas by direct velocity  
 497 measurements. *Nature*, *407*(6800), 66–69. doi: 10.1038/35024048
- 498 Le Bras, I. A.-A., Straneo, F., Holte, J., & Holliday, N. P. (2018). Season-  
 499 ality of Freshwater in the East Greenland Current System From 2014 to  
 500 2016. *Journal of Geophysical Research: Oceans*, *123*(12), 8828–8848. doi:  
 501 10.1029/2018JC014511
- 502 Lilly, J. M., Rhines, P. B., Schott, F., Lavender, K., Lazier, J., Send, U., & D’Asaro,  
 503 E. (2003, October). Observations of the Labrador Sea eddy field. *Progress in*  
 504 *Oceanography*, *59*(1), 75–176. doi: 10.1016/j.pocean.2003.08.013
- 505 Lin, P., Pickart, R. S., Torres, D. J., & Pacini, A. (2018, September). Evolution of  
 506 the Freshwater Coastal Current at the Southern Tip of Greenland. *Journal of*  
 507 *Physical Oceanography*, *48*(9), 2127–2140. doi: 10.1175/JPO-D-18-0035.1
- 508 Lozier, M. S., Li, F., Bacon, S., Bahr, F., Bower, A. S., Cunningham, S. A.,  
 509 ... Zhao, J. (2019, February). A sea change in our view of overturn-  
 510 ing in the subpolar North Atlantic. *Science*, *363*(6426), 516–521. doi:  
 511 10.1126/science.aau6592
- 512 Luo, H., Bracco, A., & Di Lorenzo, E. (2011, November). The interannual variability  
 513 of the surface eddy kinetic energy in the Labrador Sea. *Progress in Oceanogra-*  
 514 *phy*, *91*(3), 295–311. doi: 10.1016/j.pocean.2011.01.006
- 515 Luo, H., Castelao, R. M., Rennermalm, A. K., Tedesco, M., Bracco, A., Yager, P. L.,  
 516 & Mote, T. L. (2016, July). Oceanic transport of surface meltwater from  
 517 the southern Greenland ice sheet. *Nature Geoscience*, *9*(7), 528–532. doi:  
 518 10.1038/ngeo2708
- 519 Martin, T., & Biastoch, A. (2023, February). On the ocean’s response to en-  
 520 hanced Greenland runoff in model experiments: relevance of mesoscale dy-  
 521 namics and atmospheric coupling. *Ocean Science*, *19*(1), 141–167. doi:  
 522 10.5194/os-19-141-2023
- 523 Martin, T., Biastoch, A., Lohmann, G., Mikolajewicz, U., & Wang, X. (2022). On  
 524 Timescales and Reversibility of the Ocean’s Response to Enhanced Greenland  
 525 Ice Sheet Melting in Comprehensive Climate Models. *Geophysical Research*

- 526 *Letters*, 49(5), e2021GL097114. doi: 10.1029/2021GL097114
- 527 Myers, P. G., Castro de la Guardia, L., Fu, C., Gillard, L. C., Grivault, N., Hu,  
528 X., . . . Romanski, J. (2021). Extreme High Greenland Blocking Index  
529 Leads to the Reversal of Davis and Nares Strait Net Transport Toward the  
530 Arctic Ocean. *Geophysical Research Letters*, 48(17), e2021GL094178. doi:  
531 10.1029/2021GL094178
- 532 Myers, P. G., Donnelly, C., & Ribergaard, M. H. (2009, January). Structure  
533 and variability of the West Greenland Current in Summer derived from 6  
534 repeat standard sections. *Progress in Oceanography*, 80(1), 93–112. doi:  
535 10.1016/j.pocean.2008.12.003
- 536 Myers, P. G., Kulan, N., & Ribergaard, M. H. (2007). Irminger Water variability  
537 in the West Greenland Current. *Geophysical Research Letters*, 34(17). doi: 10  
538 .1029/2007GL030419
- 539 Pacini, A., & Pickart, R. S. (2022, January). Meanders of the West Greenland Cur-  
540 rent near Cape Farewell. *Deep Sea Research Part I: Oceanographic Research  
541 Papers*, 179, 103664. doi: 10.1016/j.dsr.2021.103664
- 542 Pacini, A., Pickart, R. S., Bahr, F., Torres, D. J., Ramsey, A. L., Holte, J., . . . Jong,  
543 M. F. d. (2020, September). Mean Conditions and Seasonality of the West  
544 Greenland Boundary Current System near Cape Farewell. *Journal of Physical  
545 Oceanography*, 50(10), 2849–2871. doi: 10.1175/JPO-D-20-0086.1
- 546 Pacini, A., Pickart, R. S., Bras, I. A. L., Straneo, F., Holliday, N. P., & Spall,  
547 M. A. (2021, July). Cyclonic Eddies in the West Greenland Boundary  
548 Current System. *Journal of Physical Oceanography*, 51(7), 2087–2102. doi:  
549 10.1175/JPO-D-20-0255.1
- 550 Piron, A., Thierry, V., Mercier, H., & Caniaux, G. (2016, March). Argo float ob-  
551 servations of basin-scale deep convection in the Irminger sea during winter  
552 2011–2012. *Deep Sea Research Part I: Oceanographic Research Papers*, 109,  
553 76–90. doi: 10.1016/j.dsr.2015.12.012
- 554 Piron, A., Thierry, V., Mercier, H., & Caniaux, G. (2017). Gyre-scale deep convec-  
555 tion in the subpolar North Atlantic Ocean during winter 2014–2015. *Geophys-  
556 ical Research Letters*, 44(3), 1439–1447. doi: 10.1002/2016GL071895
- 557 Rahmstorf, S., Box, J. E., Feulner, G., Mann, M. E., Robinson, A., Rutherford, S.,  
558 & Schaffernicht, E. J. (2015, May). Exceptional twentieth-century slowdown in  
559 Atlantic Ocean overturning circulation. *Nature Climate Change*, 5(5), 475–480.  
560 doi: 10.1038/nclimate2554
- 561 Rieck, J. K., Böning, C. W., & Getzlaff, K. (2019, August). The Nature of Eddy Ki-  
562 netic Energy in the Labrador Sea: Different Types of Mesoscale Eddies, Their  
563 Temporal Variability, and Impact on Deep Convection. *Journal of Physical  
564 Oceanography*, 49(8), 2075–2094. doi: 10.1175/JPO-D-18-0243.1
- 565 Rühls, S., Oliver, E. C. J., Biastoch, A., Böning, C. W., Dowd, M., Getzlaff, K., . . .  
566 Myers, P. G. (2021). Changing Spatial Patterns of Deep Convection in the  
567 Subpolar North Atlantic. *Journal of Geophysical Research: Oceans*, 126(7),  
568 e2021JC017245. doi: 10.1029/2021JC017245
- 569 Schiller-Weiss, I., Martin, T., Karstensen, J., & Biastoch, A. (2023).  
570 Do Salinity Variations Along the East Greenland Shelf Show Im-  
571 prints of Increasing Meltwater Runoff? *Journal of Geophys-  
572 ical Research: Oceans*, 128(10), e2023JC019890. (eprint:  
573 <https://onlinelibrary.wiley.com/doi/pdf/10.1029/2023JC019890>) doi:  
574 10.1029/2023JC019890
- 575 Schiller-Weiss, I., Martin, T., & Schwarzkopf, F. (2024). *Supplementary material  
576 to: Emerging impacts of enhanced greenland melting on labrador sea dynamics.*  
577 (GEOMAR Helmholtz Centre for Ocean Research Kiel [distributor] [dataset],  
578 [hdl.handle.net/20.500.12085/e3cd8f8c-07bd-4955-b77a-504377e299ac](https://hdl.handle.net/20.500.12085/e3cd8f8c-07bd-4955-b77a-504377e299ac))
- 579 Schulze Chretien, L. M., & Frajka-Williams, E. (2018, October). Wind-driven  
580 transport of fresh shelf water into the upper 30&thinsp;m of the Labrador Sea.

- 581 *Ocean Science*, *14*(5), 1247–1264. doi: 10.5194/os-14-1247-2018
- 582 Slater, T., Shepherd, A., McMillan, M., Leeson, A., Gilbert, L., Muir, A., . . . Briggs,  
583 K. (2021, November). Increased variability in Greenland Ice Sheet runoff  
584 from satellite observations. *Nature Communications*, *12*(1), 6069. (Number: 1  
585 Publisher: Nature Publishing Group) doi: 10.1038/s41467-021-26229-4
- 586 Straneo, F., Pickart, R. S., & Lavender, K. (2003, June). Spreading of Labrador sea  
587 water: an advective-diffusive study based on Lagrangian data. *Deep Sea Re-*  
588 *search Part I: Oceanographic Research Papers*, *50*(6), 701–719. doi: 10.1016/  
589 S0967-0637(03)00057-8
- 590 Sutherland, D. A., & Pickart, R. S. (2008, July). The East Greenland Coastal Cur-  
591 rent: Structure, variability, and forcing. *Progress in Oceanography*, *78*(1), 58–  
592 77. doi: 10.1016/j.pocean.2007.09.006
- 593 Swingedouw, D., Houssais, M.-N., Herbaut, C., Blaizot, A.-C., Devilliers, M., &  
594 Deshayes, J. (2022). Amoc recent and future trends: A crucial role for  
595 oceanic resolution and greenland melting? *Frontiers in Climate*, *4*. doi:  
596 10.3389/fclim.2022.838310
- 597 Tedesco, M., & Fettweis, X. (2020, April). Unprecedented atmospheric conditions  
598 (1948–2019) drive the 2019 exceptional melting season over the Greenland ice  
599 sheet. *The Cryosphere*, *14*(4), 1209–1223. doi: 10.5194/tc-14-1209-2020
- 600 Tedesco, M., Fettweis, X., Van den Broeke, M., Wal, R., Smeets, P., Berg, W., . . .  
601 Box, J. (2011, January). The role of albedo and accumulation in the 2010  
602 melting record in Greenland. *Environmental Research Letters*, *6*, 014005. doi:  
603 10.1088/1748-9326/6/1/014005
- 604 Tsujino, H., Urakawa, S., Nakano, H., Small, R. J., Kim, W. M., Yeager, S. G.,  
605 . . . Yamazaki, D. (2018, October). JRA-55 based surface dataset for driv-  
606 ing ocean–sea-ice models (JRA55-do). *Ocean Modelling*, *130*, 79–139. doi:  
607 10.1016/j.ocemod.2018.07.002
- 608 Våge, K., Pickart, R. S., Thierry, V., Reverdin, G., Lee, C. M., Petrie, B., . . . Riber-  
609 gaard, M. H. (2009, January). Surprising return of deep convection to the  
610 subpolar North Atlantic Ocean in winter 2007–2008. *Nature Geoscience*, *2*(1),  
611 67–72. doi: 10.1038/ngeo382
- 612 Yashayaev, I., Bersch, M., & van Aken, H. M. (2007). Spreading of the Labrador  
613 Sea Water to the Irminger and Iceland basins. *Geophysical Research Letters*,  
614 *34*(10). doi: 10.1029/2006GL028999
- 615 Yashayaev, I., & Clarke, A. (2008, March). Evolution of North Atlantic Water  
616 Masses Inferred from Labrador Sea Salinity Series. *Oceanography*, *21*(1), 30–  
617 45. doi: 10.5670/oceanog.2008.65
- 618 Yashayaev, I., & Loder, J. W. (2017). Further intensification of deep convection in  
619 the Labrador Sea in 2016. *Geophysical Research Letters*, *44*(3), 1429–1438. doi:  
620 10.1002/2016GL071668
- 621 Zunino, P., Mercier, H., & Thierry, V. (2020, January). Why did deep convection  
622 persist over four consecutive winters (2015–2018) southeast of Cape Farewell?  
623 *Ocean Science*, *16*(1), 99–113. doi: 10.5194/os-16-99-2020